4th International Conference on Estuaries and Coasts
8-11 October 2012, Water Resources University, *Vietnam*

ON THE HINDERED SETTLING OF SILT-WATER MIXTURES

S. te Slaa[1*], D.S. van Maren[1,2] and J.C. Winterwerp[1,2]

[1] Delft University of Technology, Faculty of Civil Engineering and Geosciences, Stevinweg 1, 2628 CN Delft, The Netherlands
[2] Deltares, PO Box 177, 2600 MH Delft, The Netherlands
[*]e-mail corresponding author: s.teslaa@gmail.com

Abstract

The sedimentation behavior of silt particles in the hindered settling regime has been considered. Therefore, laboratory experiments are carried in especially designed settling columns. Silt-water mixtures are prepared and allowed to settle at various initial concentrations. During the settling process, a continuous vertical concentration profile is measured. Settling velocities are obtained from these profiles and are compared with the widely used Richardson and Zaki (1954) expression. This comparison showed that the Richardson and Zaki expression underestimates the settling velocities for the finest silts at high concentrations. For the coarsest silt the Richardson and Zaki expression performed will with the measured data. We anticipate that this is the effect of the particle size on the apparent viscosity of the settling silt-water mixture.

Keywords: Settling velocity, settling experiment, settling column, sedimentation theory, silt

1. INTRODUCTION

Settling and bed formation of fine-grained sediment suspensions is influenced by flocculation hindered settling, and consolidation / compaction processes. Fine-grained sediments are clay, silt, and fine sands. All three size classes occur in fluvial, estuarine, and coastal systems worldwide, where often either clay or sand is dominant. Silt is defined as sediment with particle sizes (d) ranging from 2 µm to 63 µm, which has a non-cohesive base mineral, e.g. quartz or feldspar. Although silt is available in most coastal, estuarine and/or riverine systems, it is dominant in only few. China's Yellow River and Yangtze River are examples of systems where silt is abundant. Despite the obvious presence of silt in natural systems, little scientific attention has been paid to its behavior.

Consolidation processes in cohesive sediment (clay / mud) are quantitatively well understood (see e.g. Terzaghi and Fröhlich (1936), Been and Sills (1981), and Merckelbach (2000). In comparison, consolidation / compaction processes in granular beds is poorly understood even though Roberts et al. (1998) demonstrated that the density of artificial silt beds increased with time, as a result of consolidation-like processes. Sleath (1999) noted that for sand-sized material the sediment settling velocity at high concentrations is an important factor controlling the compaction of the sediment bed and the subsequent mobility. Unfortunately, both Roberts et al. (1998) and Sleath (1999) did not address the physics controlling the formation of sediment beds and the subsequent compaction or consolidation behavior. The compaction of the bed is likely to be dependent on the initial concentration of the sediment-water mixture at the onset of bed formation, for which sediment settling processes are important.

Effective settling velocities of single particles settling in an infinite fluid are well know in relation to its grain sizes (Stokes, 1851). The single-grain settling velocity may increase due to flocculation processes or decrease due to hindered settling. Flocculation processes require a clay fraction, which will not be elaborated here. Hindered settling is the reduction of sediment settling velocity at increasing sediment concentration due to grain interactions. This reduction is often parameterized with semi-empirical Richardson and Zaki (1954) (RZ) formulation for hindered settling. The RZ-formulation is derived for uniform spheres, for which the hindered settling effect is larger than for natural particles (Nielsen et al., 2002). Literature on hindered settling effects in fine sand (Qian, 1980; Wan and Wang, 1994) show no consensus on its settling behaviour. Within the fine silt range, no literature is found with respect to its settling behavior.

This paper aims to better understand and quantify the hindered settling behavior of silt. For this purpose we have done laboratory experiments which are analyzed and interpreted using existing sedimentation theory. General sedimentation theory and relevant observations of previous work will be discussed in section 2, whereas a description of the laboratory experiments is given in section 3. Section 4 presents and discusses the results of the experimental data, with final conclusions presented in section 5.

2. BACKGROUND

Framework

Hindered settling and consolidation processes, can be quantified with an integral advection-diffusion equation (see Winterwerp and Van Kesteren (2004))

$$\frac{\partial \phi_p}{\partial t} = \frac{\partial}{\partial z}\left[\Xi_s \phi_p + \left(D_s + \Gamma_T + \Gamma_c\right)\frac{\partial \phi_p}{\partial z}\right] = \frac{\partial}{\partial z}[Flux\ (\phi_p)] \qquad 1$$

here, ϕ_p the volumetric primary particle concentration of the solids fraction, D_s is the molecular diffusion coefficient, T_C is the diffusion component (i.e. consolidation coefficient), T_T is the eddy diffusivity and Ξ_s is the settling function in the advection term which consists of two parts:

$$\Xi_s = w_{s,eff} + \frac{f_c}{1+\eta f_c} \qquad 2$$

where $w_{s,eff}$ is the effective settling velocity and η is a heuristic parameter to obtain a smooth transition between the descriptions for hindered settling and consolidation. The first term in equation 2 is the particle flux in the hindered settling regime and the second term is the particle flux in the consolidation regime. The consolidation function f_c is defined by:

$$f_c = \frac{\rho_s - \rho_w}{\rho_w} k \phi_p \qquad 3$$

where ρ_s is the solid density, ρ_w is the density of water and *k* is the permeability. For silt, we infer to divide the flux in equation 1 into three phases (which may partly overlap): 1) a hindered settling phase 2) a phase of primary consolidation and 3) a phase where secondary consolidation effects due to compaction and or creep are dominant. When the diffusion term in equation 1 is small the settling function remains, therefore reducing to a 1D wave equation which can be solved with the method of characteristics. A sketch of the complete flux function is presented in Figure 1. We anticipate that fluxes in the last two phases are low compared to the first phase. The hindered settling regime ends upon reaching the critical or structural density (ρ_{struct} or $\phi_{s,struct}$). At this moment all silt particles are supported by a network structure of particles and effective stresses start to build up. In the next phase consolidation processes dominates the vertical flux which is governed by the permeability. The settling flux becomes increasingly less important and is reduced to 0 when the maximum density ($\phi_{s,\max}$) is reached.

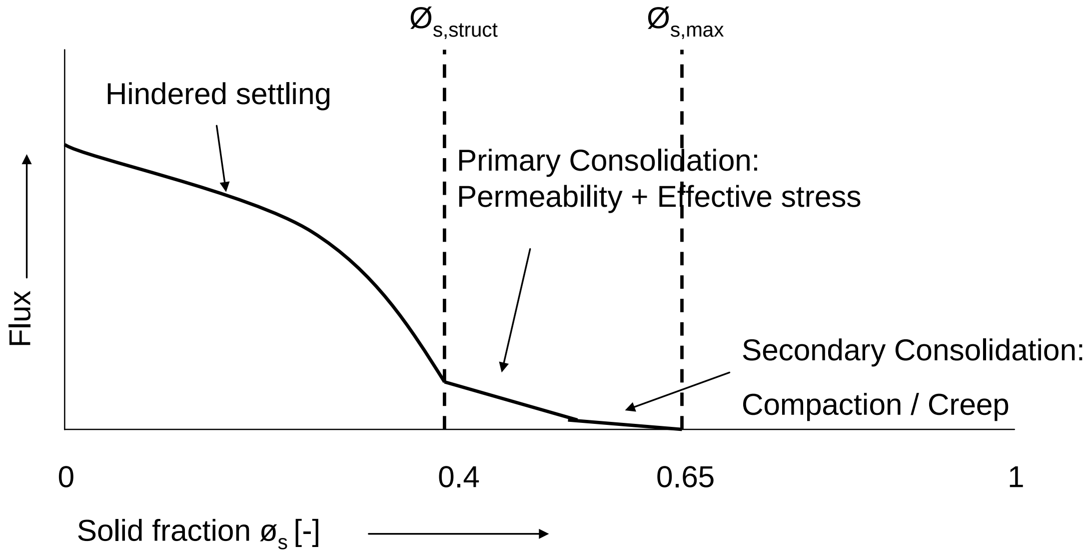

Figure 1 Sketch of the flux in equation 1 as function of ϕ_s. Three processes are incorporated in the flux: hindered settling, the generation of effect stress and the effect of compaction and/or creep.

Settling theory

In order to understand the process of sedimentation, an overview of general sedimentation mechanisms is presented first. Kynch (1952) studied the sedimentation of highly concentrated suspensions in which the settling process was determined from a continuity equation (see Dankers, 2006 for thorough elaboration on Kynch's theory). Therefore an empirical relationship between settling velocity and local sediment concentration was assumed. Sedimentation theory starts with the introduction of the vertical particle flux:

$$S = w_s \phi \tag{4}$$

In which w_s is the effective settling velocity and ϕ is the solid fraction. Hindered settling effects are introduced by assuming that effective settling velocities reduce with increasing concentration;

$$w_s = w_{s,0} f(\phi) \tag{5}$$

where f(ϕ) is a function describing the effects of concentration in the settling velocity for which f(0) = 1 and f(1) = 0. Now, the vertical one-dimensional volume balance equation can be written as:

$$\frac{\partial \phi}{\partial t} + \frac{\partial S}{\partial z} = 0 \tag{6}$$

Where t is time and z is the vertical coordinate, positive downward. Combining equations 4, 5 and 6 results in:

$$\frac{\partial \phi}{\partial t} + w_{s,0} F(\phi) \frac{\partial \phi}{\partial z} = 0 \qquad 7$$

With

$$F(\phi) = \frac{d}{d\phi}\left[\phi f(\phi)\right] \qquad 8$$

Equation 8 is a 1-D wave equation describing the settling of granular sediment-water mixtures. It is applicable in the hindered settling phase. The wave equation is hyperbolic and its solution allows for the formation of shocks. It can be solved by integrating along characteristic lines in the (*z,t*) plane. These characteristics lines are given by:

$$\frac{\mathrm{dz}}{\mathrm{d}t} = w_{s,0} F(\phi) = w_s \qquad 9$$

presenting lines of equal concentration (isolutes), where w_s is the effective settling velocity (wave speed). The height of a characteristic line is obtained by integrating equation 9. When characteristic lines converge and cross there will be a jump in concentration, called an interface. Two characteristic lines converge if $\mathrm{dz}/\mathrm{dz}_0$ decreases with time (Figure 2).

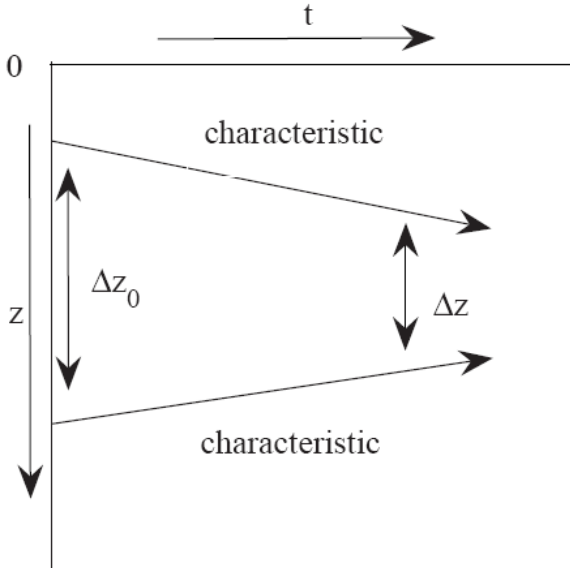

Figure 2 Two converging characteristics (Dankers, 2006)

Differentiating the equation for the height of the characteristic lines gives:

$$\frac{\mathrm{dz}}{\mathrm{dz}_0} = 1 + w_{s,0} \frac{\mathrm{d}F}{\mathrm{d}\phi} \frac{\mathrm{d}\phi}{\mathrm{dz}_0} t \qquad 10$$

Equation 10 implies that converging characteristics paths indicate the development of an interface when $\mathrm{dz}/\mathrm{dz}_0 < 0$, as $\mathrm{d}F/\mathrm{dz}_0$ is in general not negative. In settling columns, an interface will always develop between the water above the suspension and the settling suspension for mono-dispersed sediment-water mixtures. However, with increasing sediment gradation this interface becomes less pronounced due to differential settling at low concentrations. Nonetheless a lower interface will develop when characteristics in the mixture cross and it can be concluded that when $\mathrm{d}F/\mathrm{d}\phi < 0$ two interfaces develop and when $\mathrm{d}F/\mathrm{d}\phi > 0$ one interface develops. Dankers (2006) concluded that the interference between characteristics can result in a jump in concentration or a gradual change in concentration. A jump in concentration is called an interface and it can form a regular or compound shock wave. These occur when characteristic lines cross from both sides (Figure 3a, Regular type) or from one side (Figure 3b, Compound type). These two characteristic paths have 2 interfaces since $\mathrm{d}F/\mathrm{d}\phi < 0$, and hence they converge. A gradual change in concentration, in which no interface is present as the characteristics diverge, is called a rarefaction wave (Figure 3c) for which $\mathrm{d}F/\mathrm{d}\phi > 0$ indicates that characteristics converge. A regular shock wave is characteristic for the settling phase whereas rarefaction and compound waves characterizes (an early stage of) consolidation.

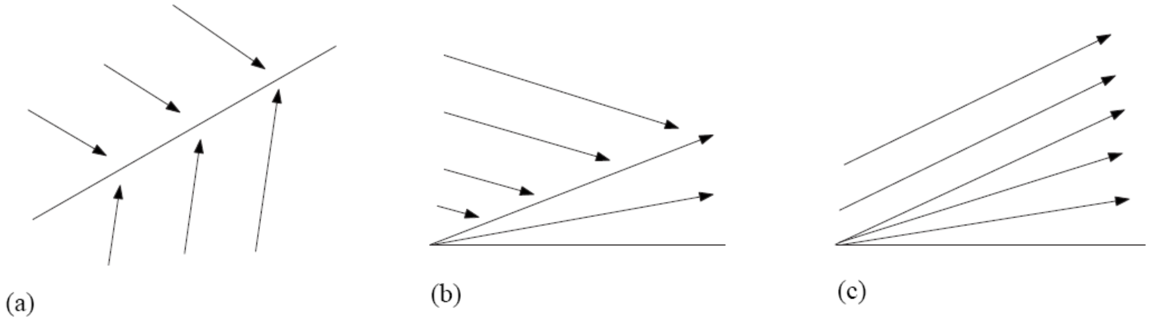

Figure 3 Three possible types of characteristic wave paths. (a) Regular type; (b) Compound type and (c) Rarefaction type after (Bartholomeeusen et al., 2003).

Hindered settling functions

Hindered settling refers to the reduced sedimentation rate of a concentrated suspensions of particles compared with the settling velocity of single particles. The type of shock that occurs depends on the sediment flux function and therefore we need to specify a hindered settling function for silt. For non-cohesive sediment, such as silt, the physical mechanisms responsible for hindered settling are return flow and wake formation around particles and an increased viscosity for the interstitial fluid. Richardson and Zaki (1954) studied these hindered settling effect using glass particles with sizes in the range of 35 µm to 1000 µm and alumina powder with a particle size of about 5 µm. They presented the nowadays commonly used semi-empirical equation for hindered settling:

$$w_s = w_{s,0}(1 - c/c_{bed})^n \qquad 11$$

Where c is the volume concentration, $w_{s,0}$ is the settling velocity of an individual particle in an infinite clear fluid and n is an empirical coefficient varying between 1 and 5 which is constant for a particular particle. Since there is no simple formulation to determine n, Baldock et al. (2004) presented an expression for n as a function of particle size for natural beach sands (200 µm < d < 1000 µm), based on fluidization experiments:

$$n = 4.4(d_{50,ref}/d_{50})^{0.2} \qquad 12$$

Where $d_{50,ref}$ = 0.2 mm, d_{50} is the median particle size. It is unclear however whether this expression is applicably outside the particle size range of their experiments. The hindered settling flux ends upon reaching c_{bed} (Figure 1). Wan and Wang (1994) also report on a dependency between n and grain size (d) based on experimental data, resulting from work done by Qian (1980). A maximum constant value for n of 4.65 for Reynolds number smaller than 0.4 and minimum values of 2.5 for Reynolds number surpassing 10^3 – 10^4 were found. Xia and Wang (1982) conducted experiments with uniform non-cohesive sand (d_{50} = 67 µm) and obtained an n-value of 7, which is larger than the maximum n-value found by Qian (1980) and larger than predicted by the formulation by Baldock et al. (2004), the latter being 5.6. Qian (1980) also performed settling experiment with non-uniform fine sand with d_{50}'s of 61 µm and 87 µm. From these experiments it was concluded that non-uniform discrete particles follow the same law as that for uniform discrete particles.

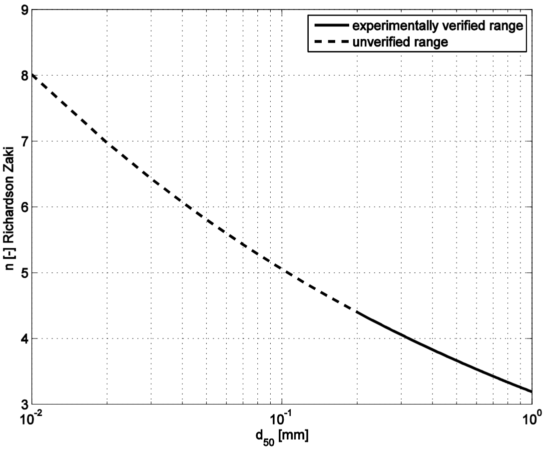

Figure 4 Variation of n, in the Richardson and Zaki (1954) hindered settling equation, as function of the d_{50} according to Baldock (2004)

We specify $f(\phi)$ in equation 5 by the RZ-formulation (11), since that is the most widely accepted hindered settling function. Now, with the theory described above the behaviour according to the hindered settling function can be predicted. Figure 5 shows the behaviour of the RZ-formulation and their derivatives (*F*) as a result of variations in *n*. In all cases, f decreases monotonically with ϕ. The derivatives all show similar behaviour, but with a different minimum critical volumetric concentration (ϕ_{cr}) representing a change in sign of $\mathrm{d}F/\mathrm{d}\phi$ from negative to positive indicating the transition from settling with two interfaces into settling with one interface. An increasing *n*-value therefore implies that this transition occurs at smaller volume concentrations. According to Baldock et. al., (2004) the *n* value increases with decreasing d_{50}, indicating that the formation of one interface occurs at lower volume concentrations. We will use this theory to analyze our experimental data in section 4.

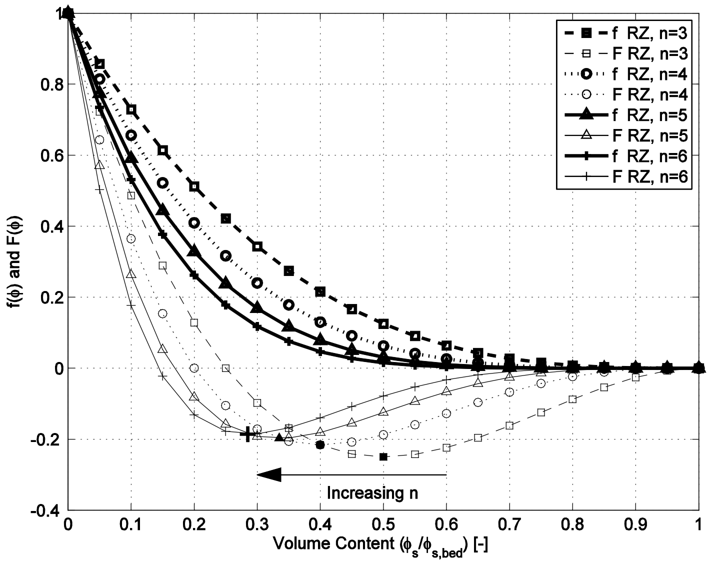

Figure 5 Variation of Richardson Zaki (1954) hindered settling functions f and F with ϕ for variation in n. Minimum values of F for carrying n are marked bold.

3. MATERIALS AND METHODS

Settling experiments are carried out in cylindrical settling columns, where silt-water mixtures are allowed to settling at varying initial concentrations. All sedimentation experiments are carried out in specially designed columns in which vertical concentration and pore water pressure profiles can be measured over time. For a complete description of these columns the reader is referred to (Te Slaa et al., 2012). Here, a short introduction to the experimental set-up will be presented:

Electrical conductivity measurements allow for a continuous measurement of a vertical density profile during a single settling experiment. At each measurement location, a measurement-port is connected to a double platinum electrode probe, mounted in the wall of the column, flush with its curvature to reduce the influence of the probes on the settling process. Each column houses 10 conductivity probes at 5, 15, 20, 25, 30, 35, 40, 45, 50 and 65 cm from the base plate. In order to correct for temperature fluctuations, the temperature of the settling mixture is measured. Temperature and conductivity measurements inside a single column are always carried out simultaneously. With this method an accuracy for ϕ_s is found to be below 0.01, corresponding with a concentration accuracy of ±26.5 g/l. In addition, pore water pressure ports are mounted in the column walls at ten intervals of 5.0 cm each, starting at 5.0 cm from the bottom. The accurate of the pressure port is ±1 mm water.

Three silt fractions are used consisting for > 99% of quartz particles with median particle sizes (d_{50}) of 14, 18 and 39 µm (Table 1). The particle size distributions are measured by laser diffraction with a Malvern particle sizer (Figure 6). Since natural fine grained sediment is less exposed to hydrodynamic sorting, gradations in natural silt sized material are large. The materials we use is wide graded ($4 < d_{90}/d_{10} < 10$) as well.

Silt #	d_{10} [µm]	d_{25} [µm]	d_{50} [µm]	d_{75} [µm]	d_{90} [µm]	d_{95} [µm]	d_{90}/d_{10} [-]
1	3	8	14	22	29	34	9.8
2	7	11	18	27	38	45	5.8
3	17	26	39	58	80	96	4.6

Table 1 Properties of particle size distribution of used silts

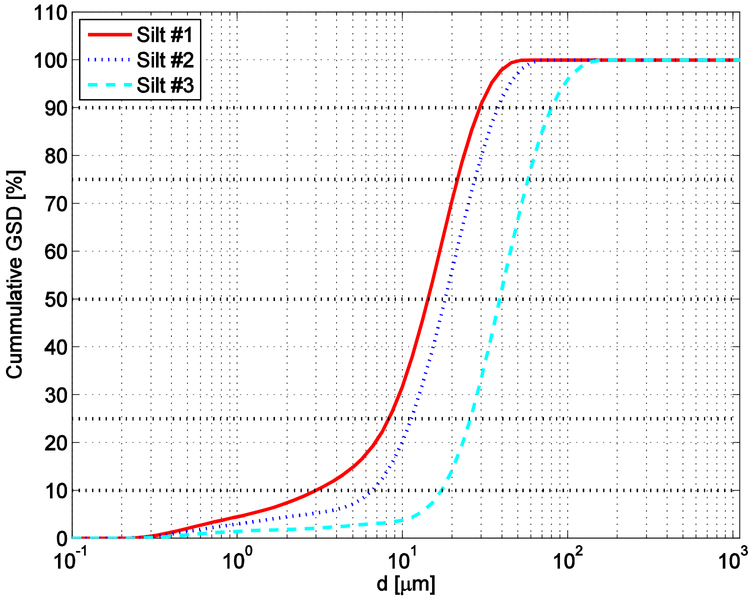

Figure 6 Particle size distributions of silts used in the sedimentation experiments

For all silt fractions, a different settling column is used in which a series of settling experiment is carried out with consecutively increasing initial sediment concentration. At the start of each experiment the silt-water mixture in the columns was homogeneously mixed, after which it was allowed to settle. In every experiment the concentration was measured at all vertical positions in the columns. When visually observed, an upper interface of the settling silt-water mixture was recorded as well.

4. RESULTS AND DISCUSSIONS

Concentration measurements

In total 33 settling experiments are carried out during which concentration profiles are measured. These profiles are used to examine settling behavior in general and the possible occurrence of shocks. Some common observations will be discussed first. Results of concentration time series for tests 5, 12 and 13 with silt 1 are presented in Figure 7. These results are characteristic for all used silt fractions. The equal concentrations at t_0, measured with all probes in a single experiment, shows that initially the silt-water mixtures are homogeneously mixed. Next, the silt particles settle and deposit on the base plate in the columns, thereby increasing the bedlevel over time. While the bed rises along a probe, the concentration, measured at this probe, increases up to the structural density. Meanwhile, the concentration measured at the probes in the overlying silt-water mixture decreases until all suspended material has settled along the corresponding probe.

Vertical concentration profiles, composed out of the concentration time series, show that concentrations increases with depth as a result of segregation (larger particles settle faster than smaller particles). The resulting vertical concentration gradient is more prominent for low sediment concentration (test 5 in Figure 7) than at high sediment concentration (tests 12 and 13 in Figure 7). This results from the range of the concentrations in the overlying silt-water mixture; the concentration gradient increases with this range. This implies that at higher concentrations segregation is reduced. The occurrence of segregation is further supported by the visual observations of sharp transitions at high concentrations and vague transitions at low sediment concentrations.

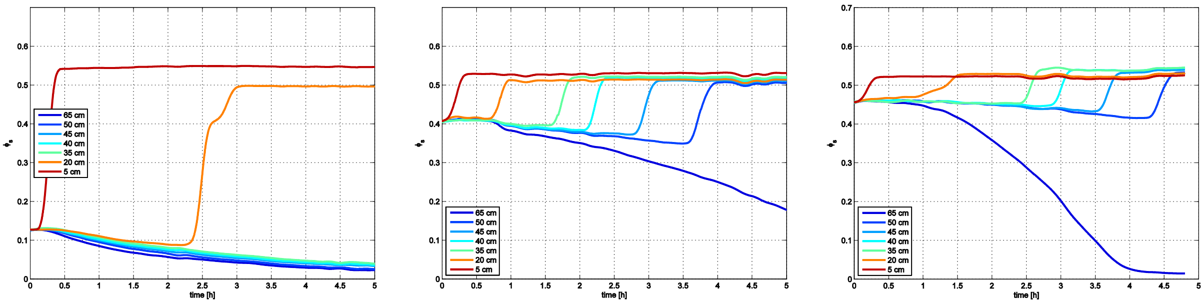

Figure 7 Concentration (ϕ_s) time series for test 5 (left, c_0 = 336 g/l), test 12 (middle, c_0 = 1054 g/l) and test 13 (right, c_0 = 1214 g/l) with silt 1. Height of the concentration measurements are indicated in the legend. The difference in duration between tests 12 and 13 before the 65 cm probe has reduced to 0 is the results of a higher water level in test 12.

Clear water settling velocity and structural density

Prior to our quantitative analyses of the hindered settling behavior of silt-water mixtures, the clear water settling velocities and maximum concentration in the settling phase (minimum concentration in the bed-phase) are determined. Clear water settling velocities ($w_{s,0}$) are computed for characteristic particles sizes (Table 2) by Stokes (1851). These velocities are later applied in order to determine hindered settling effects of concentration (Richardson and Zaki, 1954).

Silt #	**d_{10} [mm/s]**	**d_{25} [mm/s]**	**d_{50} [mm/s]**	**d_{75} [mm/s]**	**d_{90} [mm/s]**	**d_{95} [mm/s]**
1	0.008	0.062	0.184	0.420	0.780	0.9640
2	0.039	0.116	0.2970	0.679	1.301	1.067

3	0.268	0.600	1.363	2.993	5.746	8.351

Table 2 Clear water settling velocities (Stokes) for characteristic diameters of used silts

Settling velocities become zero when the volume concentration equals 1 ($\phi = 1$). This critical concentration (or structural / critical density) is obtained from the concentration measurements in our experiments at the moment of deposition. These are measured in all experiments in all silts (Figure 8). Theoretically, the minimum and maximum packing of a granular soil can be estimated from the possible arrangements of uniform spheres. The loosest packing (also know as critical or structural density) corresponds to a porosity of 47.6 % while the densest packing has a porosity of 26.0 %. For natural soils (silts and sands) the porosity generally varies between 30% and 50%, corresponding to solid fractions of 0.65 and 0.4 respectively. Figure 8 shows that the measured minimum porosities are within the range of the theoretical possible porosities. These minimum porosities are used in our further analysis as the critical density.

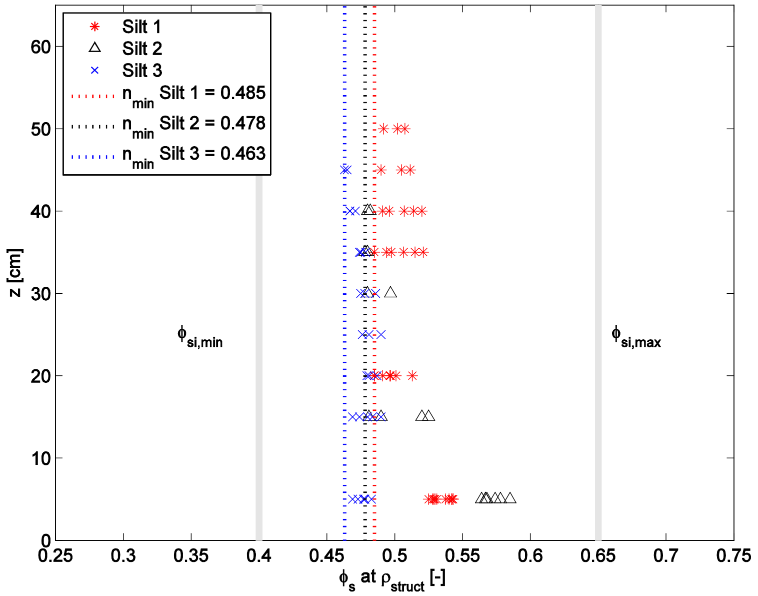

Figure 8 Measured solid fraction upon deposition at various heights in the columns for all experiments. Vertical grey lines indicate minimum and maximum solid fraction for a pure silt skeleton (Winterwerp and Van Kesteren, 2004).

Hindered settling effects

From the concentration time series measured in the settling phase (Figure 7), concentration isolines (isolutes) can be computed via vertical interpolation (Figure 9). In general, rising and descending isolutes can be distinguished. The rising isolutes represent the raising bed as a result of ongoing deposition and the descending isolutes represent settling material. The steps in the rising isolutes are the result of non-continuous measurement of the bed level since the density of the bed is measured at the moment the bed passes a probe. After deposition the isolutes are horizontal, marking complete sediment deposition and hence no consolidation on the timescale of the settling process is observed. The first time derivative of the falling isolutes provides the celerity effective settling velocity w_s, as was discussed in section 2. This celerity represents the effective settling velocity ($w_s = w_{s,0}F(\phi)$) for the magnitude of the corresponding isolute. When all descending isolutes are parallel, all particles settle at a single velocity. Normally it is not possible to draw such characteristics based on measured data in the hindered settling phase of a settling plot since the concentration in this area is the same everywhere. One should note that this does not automatically hold that parallel isolutes do not exist. Dankers (2006) already pointed out that in this area isolutes can only be determined analytically. In our experiments, only descending diverging isolutes are distinguished in the settling phase, indicating a vertical concentration gradient. The diverging character reflects a reduction of the settling velocity later in the experiment when smaller particles are left to settle.

For the lower initial concentrations (e.g. Figure 9a), the isolutes diverge stronger than for the higher initial concentration (e.g. Figure 9b), which is the result of hindered settling; at higher concentration all settling velocities are more homogeneous in a settling poly-dispersed sediment-water mixture. When the concentration within the settling silt-water mixture in a singe experiment is homogenous, isolutes are parallel and hence all material settles at a uniform velocity (plug formation?). Such behavior is observed in Figure 9c; during the first 3 hours of the experiment the only two interfaces that can be distinguished are the rising bed and the falling silt-water mixture interface. In between these interfaces the concentration is homogenous and hence no isolutes can be distinguished.

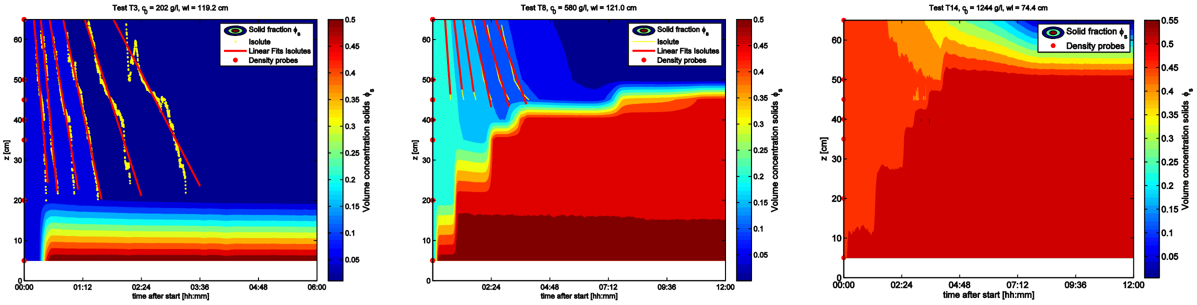

Figure 9a, b and c: Results of settling tests 3, 8 and 14 for silt #1. The slope of the computed isolutes in the hindered settling regime represents a wave celerity (settling velocity). The concentration in the area above the deposited bed is disputable due to vertical interpolation.

The computed settling velocities, resulting from the magnitude and slope of the isolutes are presented as single points in Figures 10, 11 and 12 for silts 1, 2 and 3 respectively. The connected points represent settling velocities computed within a single experiment. The largest settling velocities are measured early in the experiment when the coarsest particles are settling. Later in the experiment the finest particles are left to settling resulting in a reduction of settling velocity. As a result of segregation, the range of settling velocities within a single experiment is large at low initial concentrations. This range reduces with increasing initial concentration.

The measured settling velocities are evaluated with the RZ hindered settling formulation (equation 11) for characteristic particle sizes (d_{10}, d_{50} and d_{95}). This results in a range of settling velocities which decreases with concentration. Measured settling velocities fall well within the range of the settling velocities modeled by RZ at low concentrations. For higher concentrations however, the RZ model underestimates the measured settling velocities. It should be noted that the difference between measured and modeled settling velocities reduces with increasing particles size. For this purpose, the *n* exponent was set to 4.65, which is considered to be the maximum by Richardson and Zaki (1954). Therefore they considered the *n* value as the sum of the effects of increasing concentrations of buoyancy, return flow, apparent viscosity and wall effects on settling velocity. The apparent viscosity accounts for a factor 2.5 in the *n* exponent, which is the constant found by Einstein (1906). Winterwerp (2002) noted that for cohesive sediment the viscosity does not scale with the factor of 2.5 and therefore included the classical formula of Einstein ($\mu_{eff} = \mu_0(1+2.5\phi)$ in which μ is the viscosity) in his hindered settling equation:

$$w_s = w_{s,0}\frac{(1-\phi)(1-\phi_p)}{1+2.5\phi} \qquad 13$$

In which $\phi_p = c/\rho_s$ is the volumetric concentration of the primary particles. We compared our result in Figures 10, 11 and 12 with equation 13 as well for the same characteristic diameters. We found that the range of our measured settling velocities corresponds better with equation 13. However, now the bias between measured and modeled settling velocities increases with particles size.

Since the effects of return flow and buoyancy are soundly established in literature, we conclude that the explanation of our deviations between modeled and measured settling velocities is most likely to be found in the apparent viscosity function.

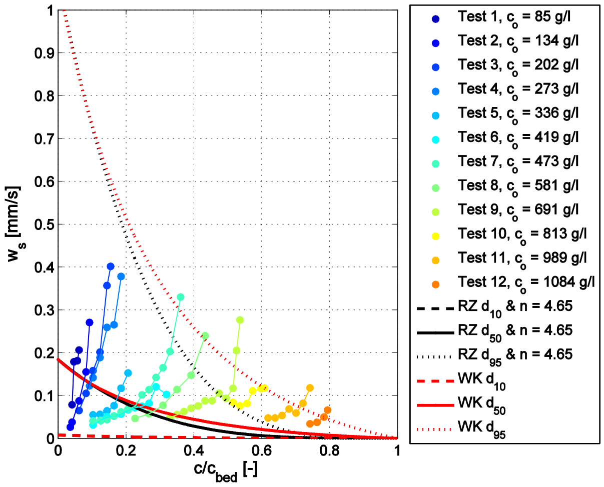

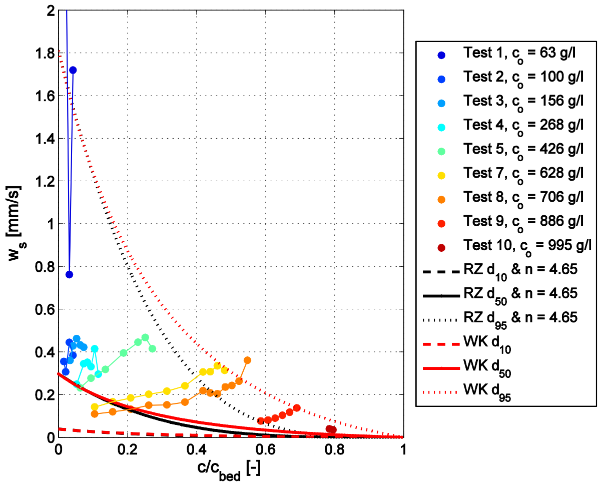

Figure 10 Settling velocities for silt 1, d_{50} = 14 μm **Figure 11 Settling velocities for silt 2, d_{50} = 18 μm**

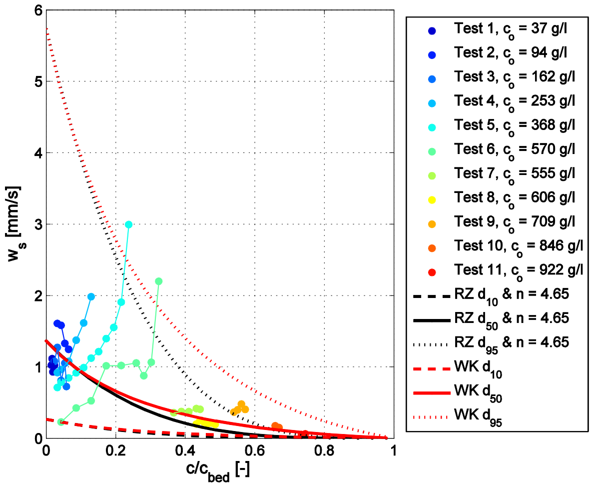

Figure 12 Settling velocities for silt 3, d_{50} = 26 μm

Consolidation

The rarefaction type of shockwave, as described in section 2, represents an increase in concentration in the sediment-water mixture below the sediment surface. Within the timescale of our experiments we did not measure a noticeable increase of the density in the bed. Therefore we conclude that consolidation does not occur on the same timescale as our settling experiments.

5. CONCLUSIONS

Settling velocities of fine silts are derived from concentration time series measurements during settling experiments. Measured settling velocities are compared with the Richardson & Zaki (1954) and Winterwerp (2002) formulations for hindered settling. The difference between these formulations finds its origin in the effect of increased viscosity on the settling velocity. For the smallest silt fraction the Richardson & Zaki formulation gives good predictions for the settling velocity at low concentration, whereas it underestimates the settling velocity at higher concentrations. The formulation by Winterwerp appears to give better result for the higher concentration. For increasing particle size however, the Richardson & Zaki formulation performs better than the Winterwerp formulation in our silts. These results indicate that there is likely an effect of particle size (in addition to concentration) on the effective viscosity as well, which is not taken into account in the Richardson & Zaki hindered settling function.

6. ACKNOWLEGEMENTS

This work has been carried as part of the Sino-Dutch collaboration project 'Effects of human activities on the eco-morphological evolution of rivers and estuaries' funded by the Dutch Royal Academy of Sciences (KNAW) and is supported by the Natural Science Foundation of China within the framework of Scientific Alliances between China and the Netherlands.

7. REFERENCES

Baldock, T.E., Tomkins, M.R., Nielsen, P. and Hughes, M.G., 2004. Settling velocity of sediments at high concentrations. Coastal Engineering, 51(1): 91-100.

Bartholomeeusen, G., De Sterck, H. and Sills, G.C., 2003. Non-convex flux functions and compound shock waves in sediment beds, *Hyperbolic Problems: Theory, Numerics, Applications: Proceedings of the Ninth International Conference on Hyperbolic Problems*, pp. 347-356.

Dankers, P.J.T., 2006. On the hindered settling of suspensions and mud-sand mixtures. Doctor Thesis Thesis, Delft University of Technology, Delft.

Einstein, A., 1906. Eine neue Bestimmung der Moleküldimensionen. Annalen der Physik, 324(2): 289-306.

Kynch, G.J., 1952. A theory of sedimentation. Transactions of the Faraday Society, 48: 166-176.

Qian, N.N.C., 1980. Preliminary study on the mechanism of hyperconcenetrated flow in north-west region of China (in Chinese). Selected papers of the symposium on sediment problems on the Yellow River, 4: 244-267.

Richardson, J.F. and Zaki, W.N., 1954. The sedimentation of a suspension of uniform spheres under conditions of viscous flow. Chemical Engineering Science, 3(2): 65-73.

Roberts, J., Jepsen, R. and Gotthard, D., 1998. Effects of particle size and bulk density on erosion of quartz particles. Journal of Hydraulic Engineering, 124: 1261.

Sleath, J.F.A., 1999. Conditions for plug formation in oscillatory flow. Continental Shelf Research, 19(13): 1643-1664.

Stokes, G.G., 1851. On the effect of the internal friction of fluids on the motion of pendulums. Transition of Cambridge Philosophy Society, 9(2): 8-106.

Te Slaa, S., He, Q., Van Maren, D.S. and Winterwerp, J.C., 2012. Sedimentation processes in silt-rich sediment mixtures, *Submitted to Ocean Dynamics*.

Wan, Z. and Wang, Z., 1994. Hyperconcentrated Flow. IAHR monograph, Balkema: Rotterdam: 230.

Winterwerp, J. and Van Kesteren, W., 2004. Introduction to the physics of cohesive sediment in the marine environment. Elsevier Science Ltd.

Winterwerp, J.C., 2002. On the flocculation and settling velocity of estuarine mud. Continental Shelf Research, 22(9): 1339-1360.

Xia, Z. and Wang, G., 1982. The settling of non-cohesive particles in a flocculated suspension (in Chinese). Journal of Sediment Research, 1: 14-23.